Insulating band gaps both below and above the Néel temperature in d-electron $LaTiO_3$, $LaVO_3$, $SrMnO_3$, and $LaMnO_3$ perovskites as a symmetry-breaking event

Oleksandr I. Malyi,* Xin-Gang Zhao, and Alex Zunger†
Renewable and Sustainable Energy Institute, University of Colorado, Boulder, Colorado 80309, USA

(Received 1 March 2023; accepted 23 May 2023; published 21 July 2023)

Metal d-electron oxides having an odd number of electrons per cell should exhibit band degeneracy at the Fermi energy, making them, in band theory, formally metallic. In many cases, however, these are false metals, as evidenced by the observation that many ABO_3 oxide perovskites with a magnetic $3d$ B atom are observed to be insulators both below and above the Néel temperature. These inconsistencies between experimental observation and expectation have historically been resolved by invoking degeneracy-breaking physics, based largely on pure electron effects, such as strong interelectronic correlation for d-electron compounds (the Mott mechanism). Such explanations generally consider the microscopic lattice or magnetic degrees of freedom (m-DOFs) as largely passive spectators, not causes of the formal metal being an insulator. However, it has long been known that ABO_3 perovskites can manifest an arrangement of m-DOFs in the form of octahedral tilting, bond dimerization, Jahn-Teller distortions, and ordering of local magnetic moments. It appears reasonable that such structural and magnetic local degrees of freedom need to be allowed to compete with purely electronic strong correlation. To answer this question, we explored a range of d-electron oxide perovskites exemplified by the archetypes $LaTiO_3$, $LaVO_3$, $SrMnO_3$, and $LaMnO_3$ with 1, 2, 3, or 4 d electrons, respectively. Using a mean-field-like electronic structure method (here, density functional theory), we find that a combination of magnetic symmetry breaking (SB) with structural distortions can account for insulating band gaps in this series while correctly predicting for the control case, an intrinsic paramagnetic metal in $SrVO_3$, as SB is insufficiently strong to remove the degeneracy. This indicates that calculating quantitatively local magnetic and positional SB motifs in unit cells that avoid averaging at the outset over the low-symmetry motifs can provide consistent trends in a Mott transition without Mott U.

DOI: 10.1103/PhysRevMaterials.7.074406

I. INTRODUCTION

Compounds that exhibit the same orbital characteristics for both filled and unfilled band edge states—for instance, when both are d-like and the number of electrons is odd—are predicted to show band degeneracy (metallic properties) at the Fermi energy level [1–4]. The conceptual usefulness of such reference systems stems from the fact that the experimentally observed systems supposed to be close to these paradigm reference have turned out to be insulators. This was the case not just for the magnetically long-range-ordered (LRO) ground-state phases [i.e., antiferromagnetic (AFM) phases below the Néel temperature] but, surprisingly, also above the Néel temperature in the paramagnetic (PM) phases, which lack magnetic LRO. Such insulating phases were seen in a range of d-electron oxide perovskites ABO_3 exemplified by the archetypes $LaTiO_3$, $LaVO_3$, $SrMnO_3$, and $LaMnO_3$ with 1, 2, 3, or 4 d electrons, respectively, contributed by the B ion, rather than the theoretically imagined false metal state [5]. This conflict has set the stage for the historical pursuit of the crucial missing ingredient in our understanding of the false metal being instead a true insulator both below and above the Néel temperature in such compounds. What made this conundrum even more intriguing was the fact that $SrVO_3$—the single d-electron isovalent analog to insulating $LaTiO_3$—has been shown to persistently be true metal at all temperatures [6,7] and that $YNiO_3$ is a true insulator in the low-T phase, becoming a true metal in the high-T phase [8].

The common textbook approach for resolving such inconsistencies between experimental observation and model expectations has followed the route of electron phases of matter, focusing largely on the role of electronic degrees of freedom (DOFs). The degeneracy breaking physics considered in such a Mott insulator with (d, d^*) band edges, for example, has focused largely on strong electron correlation, encoded, for example, by the on-site Coulomb repulsion U. When sufficiently strong, it could localize electrons, creating a (Mott) insulator instead of a false metal. The microscopic lattice DOFs (m-DOFs)—such as octahedral tilting, bond dimerization, Jahn-Teller (JT) distortions, octahedra disproportionation, and ordering of local magnetic moments—were largely considered spectator DOFs rather than the cause of the false metal reference system being actually an insulator.

This strong correlation viewpoint of gap formation is generally inaccessible to mean-field-like band structure methods, such as density functional theory (DFT). This led to the view that a strong correlation is a necessary factor needed for the

*Present address: ENSEMBLE^3 Centre of Excellence, Wolczynska 133, 01-919 Warsaw, Poland.
†Corresponding author: alex.zunger@colorado.edu

formation of real insulators from false metals. This position of the strongly correlated literature has been voiced for a long time, including very recently for the d^1, d^2, d^3, and d^4 compounds such as $LaTiO_3$ [9,10], $LaVO_3$ [11], $SrMnO_3$ [12], and $LaMnO_3$ [13], respectively. For instance, regarding $SrVO_3$ and $SrMnO_3$, Yeh *et al.* [12] indicated that "standard electronic structure methods such as DFT and GW are unable to reproduce it due to the missing correlations in their partially filled transition metal shells. The quasiparticle bandwidth in $SrVO_3$ is too wide, and $SrMnO_3$ is metallic rather than insulating". A similar impression was echoed again recently by Pavarini [13], pointing out that $LaMnO_3$ was found to be a metal in the Kohn-Sham version of DFT band theory, but it is an insulator in reality, adding, "there are entire classes of materials for which this practice fails qualitatively due to strong local electron-electron repulsion effects".

The question pondered here regards what minimal physics is needed to describe the basic trends in the phases noted above. The low-temperature LRO ground-state phases of ABO_3 are normally described by crystallographic unit cells that can geometrically accommodate nontrivial configurations of m-DOFs. The ensuing band structure calculations then reflect the electronic consequences of these m-DOFs, often representing local SB motifs. The reason that m-DOFs were often dismissed as a potential explanation of the insulating state above the Néel temperature was the tradition of describing such phases in band theory as the highest symmetry structure, after the local motifs have in fact been averaged out. Phases that lack LRO of m-DOFs such as idealized PM, paraelectric, or paraelastic phases were indeed often simplistically described by high-symmetry space groups. For example, the nominal cubic Pm-$3m$ space group common in many perovskite structures contains but a single ABO_3 repeat unit; thus, it is unable to geometrically describe symmetry breaking (SB). Band structure calculations of such high-symmetry structures cannot examine degeneracy removal by m-DOFs. However, the absence of LRO of local motifs in such phases does not mean that short-range order is absent. Avoiding the use of average, high-symmetry unit cells for paraphases or cubic phases would allow instead the possibility of a polymorphous network where a distribution of local magnetic or structural motifs would exist, should it lower the total energy. It appears reasonable that such structural and magnetic local DOFs need to be allowed to compete with purely electronic strong correlation in examining if the correct insulating vs metallic phases would emerge because of local SB. It is worth considering if the intrinsic structural and magnetic SB (present even before temperature sets in) might be related to the formation of insulating band gaps both below and above the magnetic transition, as observed in $LaTiO_3$, $LaVO_3$, $SrMnO_3$, and $LaMnO_3$. Here, we explore the outcome of such a back-and-forth ping-pong sequence where the electronic structure responds to (nonaveraged) m-DOFs, and in turn, the modified electronic landscape can reshape these m-DOF properties. To pinpoint the key factor determining whether a material is an insulator or metal in a given phase, various potential SB pathways [14] are considered. This requires avoiding the imposed high-symmetry virtual lattice averages over the local motifs both below and above the Néel temperature. Instead, each macroscopic phase is described by a supercell of its minimal cells, thereby allowing the possibility of polymorphous distribution of local motifs within the globally fixed crystallographic structure.

The main conclusions noted are:

(i) The basic metal vs insulator observed phenomenology described above is consistently predicted by mean-field-like band theory if the local positional and magnetic SB are examined. This SB predicts (a) insulating band gaps, as observed in $LaTiO_3$, $LaVO_3$, $SrMnO_3$, and $LaMnO_3$. Such insulating phases can occur in both magnetically LRO phases (below the Néel temperature) [15] and in PM phases that lack magnetic LRO [5,16–20]. (b) Additionally, the same theoretical approach applies to the control case of perovskite compounds which appear electronically and structurally indistinguishable from the d^1 insulator subgroup but in fact are observed to be persistent metals. This was found to be the case whether the relevant d orbital is a compact $3d$ (as d^1 $SrVO_3$) [6,7] or a delocalized $4d$ state (as in $SrNbO_3$ and $BaNbO_3$) [21,22]. (c) Also, the recent application of the same method to $YNiO_3$ [23] (with temperature introduced via DFT molecular dynamics) explains the prototype insulating class of below the Néel temperature and metal above it.

(ii) The distinction between this paper and the earlier works on d-electron oxide perovskites is that two local SB mechanisms—positional and magnetic—are allowed here to operate together to achieve an insulating state out of a reference zero gap metal. Comparable absolute increase in the magnitude of band gaps was noted [24–26] (in cubic, nonmagnetic (NM) and non-d-electron halide perovskites such as $CsPbX_3$, where X is a halogen). However, the initial band gap in the halide case is already nonzero.

(iii) The common belief about DFT that it cannot handle the Mott transition—a claim that has been widely exploited to introduce the dynamic mean-field theory (DMFT) [12,13]—cannot really be used for these classic $3d$ oxides as a motivation for this claim.

(iv) The physics of correcting the false metal expectation must not to rely on the on-site Coulomb repulsion Mott-Hubbard view of strong correlation. Indeed, SB allows such a Mott transition without Mott U. Thus, not having a need for U does not mean that there is no Mott-like transition to consider.

(v) As is often the case, the nature of the exchange-correlation (XC) functional in DFT can affect some results, depending on the ability of the XC to create compact orbitals. For the false metals considered in this paper, the use of advanced XC functionals such as SCAN [27] (without U as an add-on) is by itself not enough to secure a proper above-Néel insulating PM state unless one permits spin-related SB first, such as polymorphous distribution. It is essential to use an expanded supercell that enables symmetry lowering and to provide an initial nudge. Otherwise, even good XC functionals could fail qualitatively in predicting the correct metal vs insulator character.

II. METHODS: EXAMINING MAGNETIC AND STRUCTURAL SYMMETRY BREAKING BY AVOIDING THE USE OF AVERAGED CONFIGURATIONS

To describe the electronic properties of the compounds, we use symmetry-broken DFT approximation, allowing the

(a) Different degrees of symmetry breaking in $LaTiO_3$ and their effect on electronic structure

Phase	Magnetic order	Crystal structure	Magnetic SB	Structural SB	Electronic structure
Reference system	NM	Pm-3m	✗	✗	Metal (incorrect)
α	AFM	Pnma	✓	✓	Insulator
β	PM	Pm-3m	✓	✗	Metal (incorrect)
	NM	Pnma	✗	✓	Metal (incorrect)
	PM	"Pnma"	✓	✓	Insulator

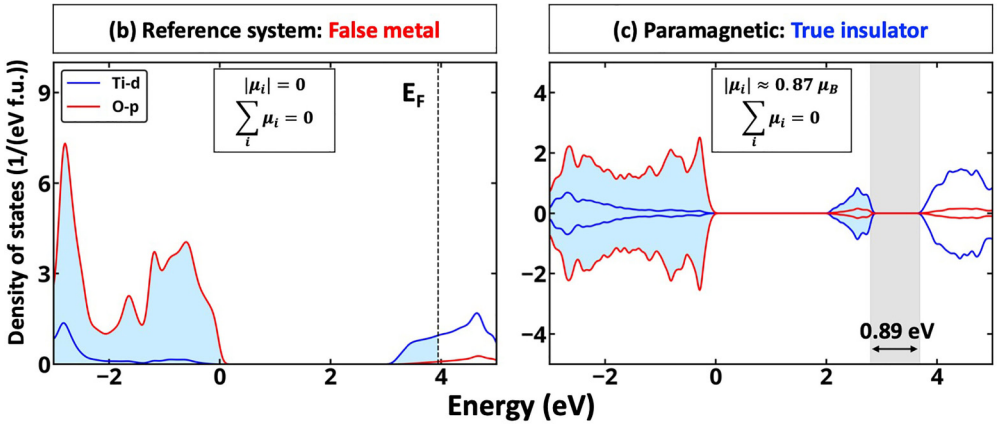

FIG. 1. (a) Summary of different degrees of symmetry breaking (SB) and their effect on the electronic structure in $LaTiO_3$. The reference system both below and above the Néel transition is defined here as a monomorphous cubic structure without any local motifs that could break symmetry, hence being a (possibly false) metal. Electronic structure of β-PM $LaTiO_3$ as described with (b) nonmagnetic and (c) spin-polymorphous models where both structural and spin SB are allowed. The results are presented for PBEsol+U with a U value of 2.5 eV. The inset show details on local and total magnetic moments in the system. The space group in quotation marks references a global average structure. Occupied states are shown as shadowed.

existence of structural and magnetic m-DOFs if their formation lowers the internal energy of the system. For magnetically ordered phases [e.g., ferromagnets (FMs) and AFMs], the lowest magnetic orders identified by Varignon *et al.* [18,19,28] are used. For the PM phases, we utilize the spin-polymorphous description—spin special quasirandom structure (SQS) [29]—which is generated for spin-up and spin-down local magnetic motifs with a global zero magnetic moment using a 160-atom supercell. Such a polymorphous description corresponds to the high-temperature limit of a random spin PM [16,30]. There are a few important consequences of the application of the spin-polymorphous model: (i) a spin-polymorphous system has significantly lower energy than a NM approximation in the system; (ii) while the NM system can often be approximated as a compound with specifically defined Wyckoff positions, the spin-polymorphous model has local structural symmetry, making each site structurally and magnetically unique; and (iii) each transition metal atom has magnetic moments. The first-principles calculations are carried out using plane-wave DFT as implemented in VASP [31–33]. The SCAN [27] meta-generalized gradient approximation functional (no $+U$ correction) or PBEsol [34] with U correction applied on d electrons of transition metals as introduced by Dudarev *et al.* [35] are used to describe XC interaction. The cutoff energies for the plane-wave basis are set to 500 eV for final calculations and 550 eV for volume relaxation. Atomic relaxations are performed until the internal forces are <0.01 eV/Å unless specified. Analysis of structural properties and visualization of computed results are performed using VESTA [36] and the Pymatgen library [37].

III. RESULTS

A. d^1 perovskite: What breaks the degeneracy creating a true insulator ($LaTiO_3$) and what retains the intrinsic metallic state ($SrVO_3$)

$LaTiO_3$ is an orthorhombic (space group: *Pnma*) insulator both below the Néel temperature ($T_N = 146$ K [38]), where it exists as the AFM α phase, and above the Néel temperature, where it exists as the PM β phase [39], in the same crystal structure [Fig. 1(a)]. With respect to the reference high-symmetry *Pm-3m* structure (not observed experimentally for $LaTiO_3$ under normal conditions), the ground-state structure has distinct symmetry lowering, inclining the TiO_6 octahedron around the $[110]_c$ axis and subsequently executing a rotation about the c axis [38]. In the strongly correlated literature [9,10], the observed insulating character of the PM β phase was argued to result from strong electron correlation—absent in band theory which incorrectly predicted this phase to be a false metal. In contrast to such a purely electronic DOF explanation, mean-field symmetry-broken polymorphous electronic structure works emphasize the effect of m-DOFs. That the α phase is insulating has been explained by the existence of AFM LRO in the presence

of energy-lowering octahedra tilting/distortion [28]. However, the fact that the PM β phase is also an insulator was initially unexpected, as this phase lacks the (spin) LRO that enabled gapping of the α phase. The transition between a low-temperature spin-ordered α phase to PM β does not necessarily involve a sudden disappearance of all local moments. Indeed, finite local moments are observed in PM phases, as evidenced by experimental measurements of magnetic pair distribution functions [40,41] or, more generally, unexpected magnetic responses of PM phases [42–49].

1. *Insulating* $LaTiO_3$*: PM within symmetry-broken polymorphous electronic structure*

For PM β $LaTiO_3$ (the same also remains for PM β $YTiO_3$), the insulating nature of the compound can be well captured by accounting for the energy-lowering structural and magnetic SB. For instance, our calculations demonstrate that the spin-polymorphous model has internal energy of 61 meV/atom, lower than that for the NM phase. Figures 1(b) and 1(c) show the density of states (DOS) of the β-PM phase in the same supercell with and without spin SB. The results show that both structural and magnetic SB is needed to describe the electronic structure of the system [i.e., magnetic or structural SB alone does not open the gap, Fig. 1(a)]. In the PM β phase, the local structural and magnetic patterns are comparable with those in the AFM α phase. However, the key difference lies in the absence of spin magnetic moment ordering. This demonstrates that, while the PM β phase shares similarities with the AFM α phase, it does not exhibit long-range spin order (as will be seen below, this is the common tendency for range of the compound discussed in this paper). Moreover, only spin SB (i.e., ignoring the structural motifs as compared with ideal high-symmetry *Pm*-3*m* perovskite structure) or only structural SB without magnetic SB (i.e., using naïve NM approximation of the PM) is not sufficient for band gap opening within DFT. These results question if DMFT predictions based on the Hamiltonian mapping of primitive cells can sufficiently capture the main physical phenomena originating from the local SB without accounting for the existence of distribution of m-DOFs.

2. *Persistent metal* d^1 $SrVO_3$ *perovskite: PM within symmetry-broken electronic structure*

This system was treated previously by the same methods as described herein [19,24] and is included for completeness. The importance of both structural and spin SB on electronic properties of PM β $LaTiO_3$ implies that, if the structural or magnetic SB is suppressed because of an intrinsic tendency of the system or, more generally, the effect of external knobs (e.g., temperature, pressure) on the material, the (d, d^*) PMs can be metallic. For instance, $SrVO_3$ (space group: *Pm*-3*m*) and $CaVO_3$ (space group: *Pnma*) are PM degenerate gapped metals with the Fermi level in the principal conduction band until the lowest temperature tried [6,7]. Both of these compounds can open the band gap due to the critical structural SB within the spin-polymorphous model [19]; however, the structural SB needed to open the gap are energetically unfavorable under normal conditions. The fact is that both $SrVO_3$ and $CaVO_3$ have a tolerance factor of close to one, which does not allow the compounds to develop sufficiently strong SB. We note, however, that using the spin-polymorphous model to describe the electronic properties of such compounds is still crucial, as accounting for the distribution of local magnetic motifs is needed to describe the electronic properties of the compounds. For instance, Wang *et al.* [24] demonstrated that the mass enhancement in $SrVO_3$ can be explained by accounting for spin SB without including any dynamic correlation effect.

B. $LaVO_3$: d^2 electron perovskite that breaks symmetry

This d^2 system was treated before (i.e., Refs. [18,19,28]), and here, we summarize the salient results to place the other d^1, d^3, and d^4 perovskites into perspective. The ground-state structure of $LaVO_3$ (α phase) is the AFM monoclinic $P2_1/b$ structure that turns into the PM orthorhombic *Pnma* structure (β phase) $\sim$140 K [50]. Both phases are insulators with confirmed JT distortion [28]. While metallic behavior is expected for $LaVO_3$ with its two electrons distributed in three t_{2g} partners, they are experimentally found to be insulators [51]. For the ground-state structure, the DFT calculations with the SCAN or PBEsol+U functional confirmed that the AFM-C magnetic configuration with monoclinic ($P2_1/b$) structure is the lowest-energy structure with band gap energy of 0.42 eV using PBEsol+U, $U = 3.5$ eV [28] or 0.78 eV using SCAN [18]. We note, however, that using soft XC functionals is unable to predict the true insulating nature [5]. The PM orthorhombic structure modeled by a monomorphous NM spin configuration based on the averaged spin structure is understandably found to be a false metal. This does not reflect a shortcoming of DFT but rather a misrepresentation of PM phases. Indeed, the NM false metal configuration has enormously higher energy (by 1167 meV/f.u.) than the spin polymorphous of the same crystallographic structure [19]. What makes $LaVO_3$ different from some other oxides is that rotations plus antipolar displacements of ions with respect to ideal Wyckoff positions in the high-symmetry cubic structure are sufficient to produce an insulating state since the Q_2^- JT mode is not important for the gap opening. We note, however, that like the β phase of $LaTiO_3$, band gap opening in both α and β phases of $LaVO_3$ requires accounting for both structural and spin SB, i.e., accounting for only one does not result in band gap opening.

C. $SrMnO_3$: d^3 electron perovskite that breaks symmetry to become an insulator

$SrMnO_3$ is an example of a (d, d^*) insulator that at low temperature exists in an AFM ordered cubic *Pm*-3*m* structure (α phase) and exhibits a Néel transition to β phase at the temperature of $\sim$260 K to a PM cubic insulator [52–54]. We note, however, that depending on synthesis conditions, AFM orthorhombic ($C222_1$), PM orthorhombic ($C222_1$), and PM tetragonal ($P6_3/mmc$) structures can be observed [55]. Recently Yeh *et al.* [12] suggested that none of the conventional theoretical approaches could obtain an insulating result for PM cubic $SrMnO_3$. Instead, exceedingly complex methods (with the self-energy embedding theory method [56–58] using GW [59] as the weakly correlated outer method for all

(a) Different degrees of symmetry breaking in $SrMnO_3$ and their effect on electronic structure

Phase	Magnetic order	Crystal structure	Magnetic SB	Structural SB	Electronic structure
Reference system	NM	Pm-3m	×	×	Metal (incorrect)
α	AFM	Pm-3m	✓	×	Insulator
β	NM	Pm-3m	×	×	Metal (incorrect)
	NM	"Pm-3m"	×	✓	Metal (incorrect)
	PM	Pm-3m	✓	×	Insulator
	PM	"Pm-3m"	✓	✓	Insulator

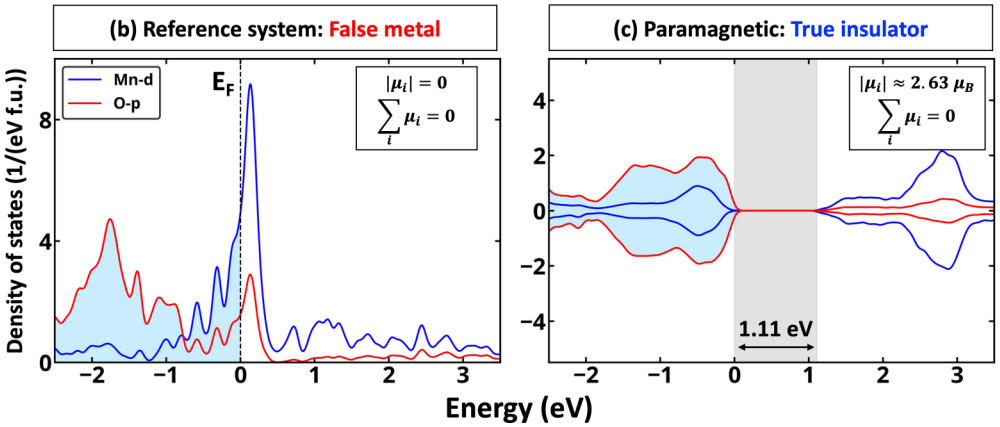

FIG. 2. (a) Summary of different degrees of symmetry breaking (SB) and their effect on the electronic structure in $SrMnO_3$. The reference system both below and above the Néel transition is defined here as a monomorphous cubic structure without any local motifs that could break symmetry. Hence, in this reference state, the system is a metal. Electronic structure of β-PM $SrMnO_3$ as described with (b) nonmagnetic and (c) spin-polymorphous models where both structural and spin SB are allowed. The results are presented for SCAN. The inset shows details on local and total magnetic moments in the system. The space group in quotation marks references the global average structure. Occupied states are shown as shadowed.

orbitals and exact diagonalization as the inner quantum impurity solver for the correlated orbitals) are required.

1. True insulating state in α and β phases of $SrMnO_3$

Using the mean-field-like DFT but without ignoring SB in describing the cubic PM phase, we observed the experimentally expected cubic PM insulating phase without accounting for any dynamic correlation. Specifically, we confirm that viewing a PM phase as one that not only has a global zero magnetization but also each atom has zero local moments (a monomorphous NM approximation) will necessarily lead to a false metallic state in a cubic phase [Fig. 2(b)]. Replacing this rather naïve monomorphous description with a polymorphous description still has the macroscopic cubic shape, but each Mn atom is not constrained to be NM, which naturally lowers the total energy and gives an insulating phase. The calculated band gap is 1.11 eV using the SCAN XC functional. The energy of the spin-polymorphous system is 460 meV/atom lower than that for the NM symmetry-unbroken description. In contrast to the monomorphous NM approximation, within the spin-polymorphous approach, we find that there is a distribution of local magnetic moments on the Mn atom with the average absolute value of magnetic moment on each side of $2.63 \pm 0.04\mu_B$. While the structural SB provided by local distortions of the individual octahedra is energy lowering, this is not the reason for the band gap opening. Without magnetic SB, the structural SB in cubic $SrMnO_3$ cannot open the gap. The band gap opening originates from the magnetic SB, which is already by itself sufficient to open the band gap. We note, however, that structural SB is still an important factor, as it can affect the absolute value of band gap energy. These results are like those found for cubic PM $CaMnO_3$ [19], where the authors demonstrated that band gap opening is due to crystal field splitting and demonstrated that crystal field splitting was strongly dependent on the degree of magnetic SB.

D. $LaMnO_3$: d^4 electron perovskite that breaks symmetry

The ground-state $LaMnO_3$ is an AFM insulator with an orthorhombic structure (α phase, *Pnma*), in which structural SB represented by octahedral tilting occurs with distinct octahedra distortion. Recently, such structural changes have been characterized as pseudo-JT distortion [28]. Upon heating, the AFM insulator turns into a PM insulator $\sim$140 K (Néel temperature) without structural phase transition (β phase, space group: *Pnma*) [60]. At a temperature >780 K, the β phase turns into the γ phase—cubic (*Pm*-3*m*) PM polaron conductors [60,61]. We note that, despite some crystallographic data confirming the phase transition, there is a clear indication of local structural SB even above the phase transition temperature in the γ phase [62].

(a) Different degrees of symmetry breaking in $LaMnO_3$ and their effect on electronic structure

Phase	Magnetic order	Crystal structure	Magnetic SB	Structural SB	Electronic structure
Reference system	NM	Pm-3m	×	×	Metal (incorrect)
α	AFM	Pnma	✓	✓	Insulator
β	NM	Pnma	×	✓	Metal (incorrect)
	PM	"Pnma"	✓	✓	Insulator
γ	PM	"Pm-3m"	✓	✓	Metal (incorrect)

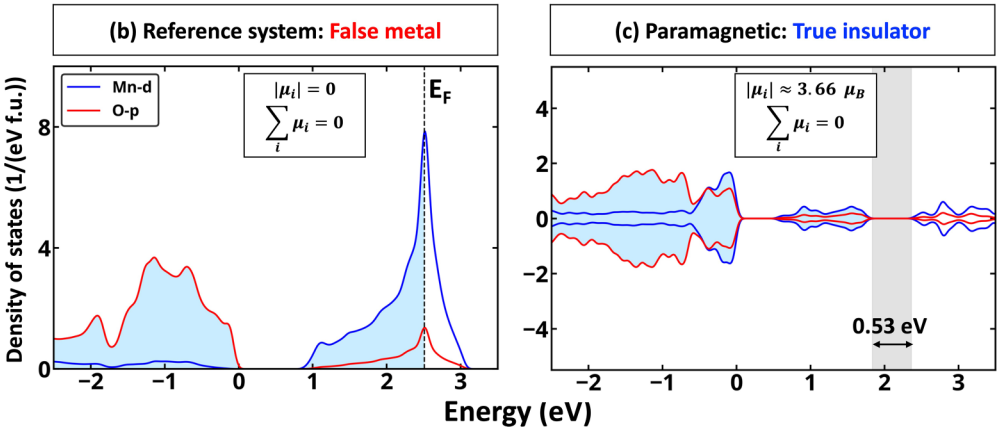

FIG. 3. (a) Summary of different degrees of symmetry breaking (SB) and their effect on the electronic structure in $LaMnO_3$. The reference system both below and above the Néel transition is defined here as a monomorphous cubic structure without any local motifs that could break symmetry. Electronic structure of β-PM $LaMnO_3$ as described with (b) nonmagnetic and (c) spin-polymorphous models where both structural and spin SB are allowed. The results are presented for SCAN. The inset shows details on local and total magnetic moments in the system. The space group in quotation marks references the global average structure. Occupied states are shown as shadowed.

1. True insulating state in α and β phases and true metallic state of γ phase of $LaMnO_3$

For the orthorhombic α phase of $LaMnO_3$, by using AFM configuration, we indeed find the insulating state with SCAN band gap 0.49 eV [see Fig. 3(a)]. These results are consistent with previous experimental and theoretical results [18,19,28]. Moreover, the calculated local spin moment on the Mn atom is $3.66\mu_B$, close to the value measured in the experiment ($3.7\ \mu_B$) [63]. We note that the description of the insulating state in the α phase requires accounting for structural distortion present in the orthorhombic phase. If the α phase is approximated as an ideal high-symmetry *Pm*-3*m* structure (i.e., one often used in the correlation models), the magnetic SB (i.e., AFM) is unable to open the gap. These results thus clearly highlight the importance of structural SB (specifically pseudo-JT distortion) in the band gap opening.

While the origin of band gap opening in the α phase of $LaMnO_3$ is rather well understood, historically, the β phase attracted the most interest in the literature on correlated materials [13]; using global average NM configuration (zero spin moment on each Mn atom), it is found to be a false metal. Hence, the inability to describe the insulating state of the β phase of $LaMnO_3$ within naïve DFT approximation historically has been used as motivation to develop post-DFT methods (like DMFT). For the β phase, the spin-polymorphous model can describe the insulating state when structural and magnetic SB is accounted for [Figs. 3(a) and 3(b)]. The spin-polymorphous system has the distribution of local magnetic moments in the Mn site with a magnetic moment of $3.66 \pm 0.01\ \mu_B$ and substantially lower internal energy (as compared with the naïve NM approximation of the PM). These results thus demonstrate that the gapping of the β phase can be described by the accounting of the formation of m-DOFs that lower internal energy without accounting for any dynamic correlation. Importantly, in contrast to cubic PM $SrMnO_3$, accounting for only one m-DOF (i.e., structural SB or magnetic SB) is insufficient to open the gap [Fig. 3(a)].

What makes the case of $LaMnO_3$ interesting is the fact that the γ phase is metallic with spin and structure SB accounted for [see Fig. 3(a)], which is in good agreement with experimentally observed polaron conductor behavior [60,61]. Since the Mn magnetic moments for the γ and β phases are close ($3.63\ \mu_B$ for the former and $3.66\ \mu_B$ for the latter), we conclude that insulating states (like the cases of PM $SrVO_3$ and $CaVO_3$) need sufficient structure SB seen in the β phase which is, however, not developed in γ phase of $LaMnO_3$ as the result of energy-lowering formation of m-DOFs.

IV. SUMMARY AND DISCUSSION

We have demonstrated that the electronic properties of $LaTiO_3$, $LaVO_3$, $SrMnO_3$, and $LaMnO_3$ compounds, previously referred to as false metals, can be described using DFT both below and above the Néel temperature. Specifically, such an accurate description requires consideration of three key factors:

(i) One should not use the average unit cell. Instead, we should expand it to a supercell with spin and structural SQS, which permits more DOFs. For instance, for materials like $LaTiO_3$ and $LaVO_3$, acknowledging this spin and structural symmetry disruption lets us articulate their insulating characteristics. Similarly, the insulating state in the β phase of $LaMnO_3$ can be characterized when factoring in the spin and structural SB.

(ii) We should consider advanced XC functional usage. While in this paper, we do not prioritize establishing the superiority of SCAN or PBEsol+U in calculating the electronic properties of the discussed compounds, we demonstrate that they, along with others like hybrid [64–67] or r^{2}SCAN [68] functionals, can yield accurate electronic structures if they allow for energy-lowering symmetry disruptions.

(iii) There should be an allowance for collaboration between different modes of microscopic DOFs. For instance, in $SrMnO_3$, the band gap opening stems from the magnetic symmetry disruption, while the structural symmetry disruption modifies the overall band gap energy value.

This three-pronged approach not only allows us to reproduce the Néel temperature for PM materials [30] accurately and describe the metal-insulator transition [23] when the weakening of structural symmetry disruption due to temperature is considered. Furthermore, it also provides a thorough understanding of the electronic properties of these materials without the necessity for more complex post-DFT methods. The dataset of materials discussed here is limited, but it emphasizes that a polymorphous network and its influence on the electronic properties of quantum materials is a broad topic. Therefore, it is critical to avoid making premature conclusions about strong electron-electron correlation in pseudometal syndrome cases. Instead, the three-pronged strategy we propose—namely, expanding to a supercell, utilizing advanced XC functionals, and allowing collaborations between different modes of microscopic DOFs—can satisfactorily explain the lack of false metals in numerous cases.

ACKNOWLEDGMENTS

The work on magnetic symmetry breaking and electronic structure calculations was supported by the U.S. Department of Energy (DOE), Office of Science, Basic Energy Sciences, Materials Sciences and Engineering Division within Grant No. DE-SC0010467 to CU Boulder, while using resources of the National Energy Research Scientific Computing Center, which is supported by the Office of Science of the DOE. The authors also acknowledge use of computational resources located at the National Renewable Energy Laboratory and sponsored by the DOE's Office of Energy Efficiency and Renewable Energy for optimization of perovskite polymorphous crystal structures. Work on structural symmetry breaking was done with the support of NSF-DMREF Grant No. 1921949.

[1] J. H. d. Boer and E. J. W. Verwey, Semi-conductors with partially and with completely filled 3d-lattice bands, Proc. Phys. Soc. **49**, 59 (1937).

[2] N. F. Mott, The basis of the electron theory of metals, with special reference to the transition metals, Proc. Phys. Soc. A **62**, 416 (1949).

[3] N. F. Mott and R. Peierls, Discussion of the paper by de Boer and Verwey, Proc. Phys. Soc. **49**, 72 (1937).

[4] J. Hubbard, Electron correlations in narrow energy bands, Proc. R. Soc. Lond. A **276**, 238 (1963).

[5] O. I. Malyi and A. Zunger, False metals, real Insulators, and degenerate gapped metals, Appl. Phys. Rev. **7**, 041310 (2020).

[6] L. Zhang, Y. J. Zhou, L. Guo, W. W. Zhao, A. Barnes, H. T. Zhang, C. Eaton, Y. X. Zheng, M. Brahlek, H. F. Haneef *et al.*, Correlated metals as transparent conductors, Nat. Mater. **15**, 204 (2016).

[7] M. Takizawa, M. Minohara, H. Kumigashira, D. Toyota, M. Oshima, H. Wadati, T. Yoshida, A. Fujimori, M. Lippmaa, M. Kawasaki *et al.*, Coherent and incoherent d band dispersions in $SrVO_3$, Phys. Rev. B **80**, 235104 (2009).

[8] J. A. Alonso, J. L. García-Muñoz, M. T. Fernández-Díaz, M. A. G. Aranda, M. J. Martínez-Lope, and M. T. Casais, Charge Disproportionation in $RNiO_3$ Perovskites: Simultaneous Metal-Insulator and Structural Transition in $YNiO_3$, Phys. Rev. Lett. **82**, 3871 (1999).

[9] E. Pavarini, S. Biermann, A. Poteryaev, A. I. Lichtenstein, A. Georges, and O. K. Andersen, Mott Transition and Suppression of Orbital Fluctuations in Orthorhombic 3d^1 Perovskites, Phys. Rev. Lett. **92**, 176403 (2004).

[10] E. Pavarini, A. Yamasaki, J. Nuss, and O. K. Andersen, How chemistry controls electron localization in 3d^1 perovskites: A Wannier-function study, New J. Phys. **7**, 188 (2005).

[11] M. De Raychaudhury, E. Pavarini, and O. K. Andersen, Orbital Fluctuations in the Different Phases of $LaVO_3$ and YVO_3, Phys. Rev. Lett. **99**, 126402 (2007).

[12] C.-N. Yeh, S. Iskakov, D. Zgid, and E. Gull, Electron correlations in the cubic paramagnetic perovskite Sr(V, Mn)O_3: Results from fully self-consistent self-energy embedding calculations, Phys. Rev. B **103**, 195149 (2021).

[13] E. Pavarini, Solving the strong-correlation problem in materials, Riv. Nuovo Cim. **44**, 597 (2021).

[14] A. Zunger, Bridging the gap between density functional theory and quantum materials, Nat. Comput. Sci. **2**, 529 (2022).

[15] J. Varignon, O. I. Malyi, and A. Zunger, Dependence of band gaps in d-electron perovskite oxides on magnetism, Phys. Rev. B **105**, 165111 (2022).

[16] D. Gambino, O. I. Malyi, Z. Wang, B. Alling, and A. Zunger, Density functional description of spin, lattice, and spin-lattice dynamics in antiferromagnetic and paramagnetic phases at finite temperatures, Phys. Rev. B **106**, 134406 (2022).

[17] O. I. Malyi, X.-G. Zhao, A. Bussmann-Holder, and A. Zunger, Local positional and spin symmetry breaking as a source of magnetism and insulation in paramagnetic $EuTiO_3$, Phys. Rev. Mater. **6**, 034604 (2022).

[18] J. Varignon, M. Bibes, and A. Zunger, Mott gapping in 3d ABO_3 perovskites without Mott-Hubbard interelectronic repulsion energy U, Phys. Rev. B **100**, 035119 (2019).

[19] J. Varignon, M. Bibes, and A. Zunger, Origin of band gaps in 3*d* perovskite oxides, Nat. Commun. **10**, 1658 (2019).

[20] G. Trimarchi, Z. Wang, and A. Zunger, Polymorphous band structure model of gapping in the antiferromagnetic and paramagnetic phases of the Mott insulators MnO, FeO, CoO, and NiO, Phys. Rev. B **97**, 035107 (2018).

[21] X. Xu, C. Randorn, P. Efstathiou, and J. T. S. Irvine, A red metallic oxide photocatalyst, Nat. Mater. **11**, 595 (2012).

[22] M. T. Casais, J. A. Alonso, I. Rasines, and M. A. Hidalgo, Preparation, neutron structural study and characterization of $BaNbO_3$—a Pauli-like metallic perovskite, Mater. Res. Bull. **30**, 201 (1995).

[23] O. I. Malyi and A. Zunger, Rise and fall of Mott insulating gaps in $YNiO_3$ paramagnets as a reflection of symmetry breaking and remaking, Phys. Rev. Mater. **7**, 044409 (2023).

[24] Z. Wang, O. I. Malyi, X. Zhao, and A. Zunger, Mass enhancement in 3*d* and $s-p$ perovskites from symmetry breaking, Phys. Rev. B **103**, 165110 (2021).

[25] X.-G. Zhao, Z. Wang, O. I. Malyi, and A. Zunger, Effect of static local distortions vs. dynamic motions on the stability and band gaps of cubic oxide and halide perovskites, Mater. Today **49**, 107 (2021).

[26] X.-G. Zhao, G. M. Dalpian, Z. Wang, and A. Zunger, Polymorphous nature of cubic halide perovskites, Phys. Rev. B **101**, 155137 (2020).

[27] J. Sun, A. Ruzsinszky, and J. P. Perdew, Strongly Constrained and Appropriately Normed Semilocal Density Functional, Phys. Rev. Lett. **115**, 036402 (2015).

[28] J. Varignon, M. Bibes, and A. Zunger, Origins versus fingerprints of the Jahn-Teller effect in *d*-electron ABX_3 perovskites, Phys. Rev. Res. **1**, 033131 (2019).

[29] A. Zunger, S. H. Wei, L. G. Ferreira, and J. E. Bernard, Special Quasirandom Structures, Phys. Rev. Lett. **65**, 353 (1990).

[30] J. L. Du, O. I. Malyi, S. L. Shang, Y. Wang, X. G. Zhao, F. Liu, A. Zunger, and Z. K. Liu, Density functional thermodynamic description of spin, phonon and displacement degrees of freedom in antiferromagnetic-to-paramagnetic phase transition in $YNiO_3$, Mater. Today Phys. **27**, 100805 (2022).

[31] G. Kresse and J. Hafner, *Ab initio* molecular dynamics for liquid metals, Phys. Rev. B **47**, 558 (1993).

[32] G. Kresse and J. Furthmüller, Efficiency of *ab-initio* total energy calculations for metals and semiconductors using a plane-wave basis set, Comput. Mater. Sci. **6**, 15 (1996).

[33] G. Kresse and J. Furthmüller, Efficient iterative schemes for *ab initio* total-energy calculations using a plane-wave basis set, Phys. Rev. B **54**, 11169 (1996).

[34] J. P. Perdew, A. Ruzsinszky, G. I. Csonka, O. A. Vydrov, G. E. Scuseria, L. A. Constantin, X. Zhou, and K. Burke, Restoring the Density-Gradient Expansion for Exchange in Solids and Surfaces, Phys. Rev. Lett. **100**, 136406 (2008).

[35] S. L. Dudarev, G. A. Botton, S. Y. Savrasov, C. J. Humphreys, and A. P. Sutton, Electron-energy-loss spectra and the structural stability of nickel oxide: An LSDA+U study, Phys. Rev. B **57**, 1505 (1998).

[36] K. Momma and F. Izumi, VESTA 3 for three-dimensional visualization of crystal, volumetric and morphology data, J. Appl. Crystallogr. **44**, 1272 (2011).

[37] S. P. Ong, W. D. Richards, A. Jain, G. Hautier, M. Kocher, S. Cholia, D. Gunter, V. L. Chevrier, K. A. Persson, and G. Ceder, Python Materials Genomics (Pymatgen): A robust, open-source python library for materials analysis, Comput. Mater. Sci. **68**, 314 (2013).

[38] M. Cwik, T. Lorenz, J. Baier, R. Müller, G. André, F. Bourée, F. Lichtenberg, A. Freimuth, R. Schmitz, E. Müller-Hartmann *et al.*, Crystal and magnetic structure of $LaTiO_3$: Evidence for nondegenerate t_{2g} orbitals, Phys. Rev. B **68**, 060401(R) (2003).

[39] J. Hemberger, H. A. K. von Nidda, V. Fritsch, J. Deisenhofer, S. Lobina, T. Rudolf, P. Lunkenheimer, F. Lichtenberg, A. Loidl, D. Bruns *et al.*, Evidence for Jahn-Teller Distortions at the Distortions at the Antiferromagnetic Transition in $LaTO_3$, Phys. Rev. Lett. **91**, 066403 (2003).

[40] B. Frandsen, X. Yang, and S. J. Billinge, Magnetic pair distribution function analysis of local magnetic correlations, Acta Cryst. A **70**, 3 (2014).

[41] B. A. Frandsen, M. Brunelli, K. Page, Y. J. Uemura, J. B. Staunton, and S. J. L. Billinge, Verification of Anderson Superexchange in MnO Via Magnetic Pair Distribution Function Analysis and *Ab Initio* Theory, Phys. Rev. Lett. **116**, 197204 (2016).

[42] Z. Guguchia, H. Keller, R. K. Kremer, J. Köhler, H. Luetkens, T. Goko, A. Amato, and A. Bussmann-Holder, Spin-lattice coupling induced weak dynamical magnetism in $EuTiO_3$ at high temperatures, Phys. Rev. B **90**, 064413 (2014).

[43] Z. Guguchia, H. Keller, J. Köhler, and A. Bussmann-Holder, Magnetic field enhanced structural instability in $EuTiO_3$, J. Phys.: Condens. Matter **24**, 492201 (2012).

[44] A. Bussmann-Holder, J. Köhler, K. Roleder, Z. Guguchia, and H. Keller, Unexpected magnetism at high temperature and novel magneto-dielectric-elastic coupling in $EuTiO_3$: A critical review, Thin. Solid. Films **643**, 3 (2017).

[45] G. Gregori, J. Köhler, J. F. Scott, and A. Bussmann-Holder, Hidden magnetism in the paramagnetic phase of $EuTiO_3$, J. Phys.: Condens. Matter **27**, 496003 (2015).

[46] Z. Guguchia, Z. Salman, H. Keller, K. Roleder, J. Köhler, and A. Bussmann-Holder, Complexity in the structural and magnetic properties of almost multiferroic $EuTiO_3$, Phys. Rev. B **94**, 220406(R) (2016).

[47] P. Pappas, M. Calamiotou, M. Polentarutti, G. Bais, A. Bussmann-Holder, and E. Liarokapis, Magnetic field driven novel phase transitions in $EuTiO_3$, J. Phys.: Condens. Matter **34**, 02LT01 (2021).

[48] T. Katsufuji and H. Takagi, Coupling between magnetism and dielectric properties in quantum paraelectric $EuTiO_3$, Phys. Rev. B **64**, 054415 (2001).

[49] A. Bussmann-Holder, Z. Guguchia, J. Köhler, H. Keller, A. Shengelaya, and A. R. Bishop, Hybrid paramagnon phonon modes at elevated temperatures in $EuTiO_3$, New J. Phys. **14**, 093013 (2012).

[50] D. J. Lovinger, M. Brahlek, P. Kissin, D. M. Kennes, A. J. Millis, R. Engel-Herbert, and R. D. Averitt, Influence of spin and orbital fluctuations on Mott-Hubbard exciton dynamics in $LaVO_3$ thin films, Phys. Rev. B **102**, 115143 (2020).

[51] S. Miyasaka, Y. Okimoto, M. Iwama, and Y. Tokura, Spin-orbital phase diagram of perovskite-type RVO_3 ($R =$ rare $-$ earth ion or Y), Phys. Rev. B **68**, 100406(R) (2003).

[52] O. Chmaissem, B. Dabrowski, S. Kolesnik, J. Mais, J. D. Jorgensen, and S. Short, Structural and magnetic phase diagrams of $La_{1-x}Sr_xMnO_3$ and $Pr_{1-y}Sr_yMnO_3$, Phys. Rev. B **67**, 094431 (2003).

[53] R. K. Hona and F. Ramezanipour, Effect of the oxygen vacancies and structural order on the oxygen evolution activity: A case study of $SrMnO_{3-\delta}$ featuring four different structure types, Inorg. Chem. **59**, 4685 (2020).

[54] T. Takeda and S. Ōhara, Magnetic structure of the cubic perovskite self-energy embedding theory (SEET) for periodic systems type $SrMnO_3$, J. Phys. Soc. Jpn. **37**, 275 (1974).

[55] A. Daoud-Aladine, C. Martin, L. C. Chapon, M. Hervieu, K. S. Knight, M. Brunelli, and P. G. Radaelli, Structural phase transition and magnetism in hexagonal $SrMnO_3$ by magnetization measurements and by electron, x-ray, and neutron diffraction studies, Phys. Rev. B **75**, 104417 (2007).

[56] A. A. Kananenka, E. Gull, and D. Zgid, Systematically improvable multiscale solver for correlated electron systems, Phys. Rev. B **91**, 121111(R) (2015).

[57] D. Zgid and E. Gull, Finite temperature quantum embedding theories for correlated systems, New J. Phys. **19**, 023047 (2017).

[58] A. A. Rusakov, S. Iskakov, L. N. Tran, and D. Zgid, Self-energy embedding theory (SEET) for periodic systems, J. Chem. Theory Comput. **15**, 229 (2019).

[59] F. Aryasetiawan and O. Gunnarsson, The GW method, Rep. Prog. Phys. **61**, 237 (1998).

[60] Y. Murakami, J. P. Hill, D. Gibbs, M. Blume, I. Koyama, M. Tanaka, H. Kawata, T. Arima, Y. Tokura, K. Hirota *et al.*, Resonant X-Ray Scattering from Orbital Ordering in $LaMnO_3$, Phys. Rev. Lett. **81**, 582 (1998).

[61] J. S. Zhou and J. B. Goodenough, Paramagnetic phase in single-crystal $LaMnO_3$, Phys. Rev. B **60**, R15002(R) (1999).

[62] X. Qiu, T. Proffen, J. F. Mitchell, and S. J. L. Billinge, Orbital Correlations in the Pseudocubic O and Rhombohedral R Phases of $LaMnO_3$, Phys. Rev. Lett. **94**, 177203 (2005).

[63] J. B. A. A. Elemans, B. Van Laar, K. R. Van Der Veen, and B. O. Loopstra, The crystallographic and magnetic structures of $La_{1-x}Ba_xMn_{1-x}Me_xO_3$ (Me = Mn or Ti), J. Solid State Chem. **3**, 238 (1971).

[64] Y. Jiao, E. Schröder, and P. Hyldgaard, Extent of Fock-exchange mixing for a hybrid van der Waals density functional? J. Chem. Phys. **148**, 194115 (2018).

[65] V. Shukla, Y. Jiao, J.-H. Lee, E. Schröder, J. B. Neaton, and P. Hyldgaard, Accurate Nonempirical Range-Separated Hybrid van der Waals Density Functional for Complex Molecular Problems, Solids, and Surfaces, Phys. Rev. X **12**, 041003 (2022).

[66] J. Heyd, G. E. Scuseria, and M. Ernzerhof, Hybrid functionals based on a screened Coulomb potential, J. Chem. Phys. **118**, 8207 (2003).

[67] A. V. Krukau, O. A. Vydrov, A. F. Izmaylov, and G. E. Scuseria, Influence of the exchange screening parameter on the performance of screened hybrid functionals, J. Chem. Phys. **125**, 224106 (2006).

[68] J. W. Furness, A. D. Kaplan, J. Ning, J. P. Perdew, and J. Sun, Accurate and numerically efficient r^2SCAN meta-generalized gradient approximation, J. Phys. Chem. Lett. **11**, 8208 (2020).